

FORMATION OF FULLERENES IN H-CONTAINING PLANETARY NEBULAE

D. A. GARCÍA-HERNÁNDEZ^{1,2}, A. MANCHADO^{1,2,3}, P. GARCÍA-LARIO⁴, L. STANGHELLINI⁵,
E. VILLAYER⁶, R. A. SHAW⁵, R. SZCZERBA⁷, AND J. V. PEREA-CALDERÓN⁸

¹ Instituto de Astrofísica de Canarias, C/Vía Láctea s/n, 38200 La Laguna, Spain; agarcia@iac.es, amt@iac.es

² Departamento de Astrofísica, Universidad de La Laguna (ULL), E-38205 La Laguna, Spain

³ Consejo Superior de Investigaciones Científicas, Spain

⁴ Herschel Science Centre, European Space Astronomy Centre, Research and Scientific Support Department of ESA, Villafraanca del Castillo, P.O. Box 50727, E-28080 Madrid, Spain; Pedro.Garcia-Lario@sciops.esa.int

⁵ National Optical Astronomy Observatory, 950 North Cherry Avenue, Tucson, AZ 85719, USA; shaw@noao.edu, letizia@noao.edu

⁶ Departamento de Física Teórica C-XI, Universidad Autónoma de Madrid, E-28049 Madrid, Spain; eva.villaver@uam.es

⁷ N. Copernicus Astronomical Center, Rabiańska 8, 87-100 Toruń, Poland; szczerba@ncac.torun.pl

⁸ European Space Astronomy Centre, INSA S. A., P.O. Box 50727, E-28080 Madrid, Spain; Jose.Perea@sciops.esa.int

Received 2010 August 10; accepted 2010 September 21; published 2010 October 28

ABSTRACT

Hydrogen depleted environments are considered an essential requirement for the formation of fullerenes. The recent detection of C₆₀ and C₇₀ fullerenes in what was interpreted as the hydrogen-poor inner region of a post-final helium shell flash planetary nebula (PN) seemed to confirm this picture. Here, we present strong evidence that challenges the current paradigm regarding fullerene formation, showing that it can take place in circumstellar environments containing hydrogen. We report the simultaneous detection of polycyclic aromatic hydrocarbons (PAHs) and fullerenes toward C-rich and H-containing PNe belonging to environments with very different chemical histories such as our own Galaxy and the Small Magellanic Cloud. We suggest that PAHs and fullerenes may be formed by the photochemical processing of hydrogenated amorphous carbon. These observations suggest that modifications may be needed to our current understanding of the chemistry of large organic molecules as well as the chemical processing in space.

Key words: astrochemistry – circumstellar matter – infrared: stars – planetary nebulae: general – stars: AGB and post-AGB

Online-only material: color figures

1. INTRODUCTION

The current understanding of the fullerene formation is that it is inhibited by the presence of hydrogen (De Vries et al. 1993; Wang et al. 1995; Cherchneff et al. 2000; Jäger et al. 2009) and as laboratory experiments show it is extremely efficient as graphite is vaporized in hydrogen-deficient atmospheres with helium as buffer gas (Kroto et al. 1985; Kratschmer et al. 1990). As a consequence, fullerene molecules in astrophysical domains are expected to be efficiently formed in hot (>3500 K), hydrogen-poor, and C-rich environments such as Wolf-Rayet (W-R) stars (Cherchneff et al. 2000; Jäger et al. 2009) or extremely hydrogen-deficient objects such as the R Coronae Borealis stars (Goeres & Sedlmayr 1992). In such conditions, fullerenes are thought to be built from the coalescence of large monocyclic rings in the gas phase (Cherchneff et al. 2000) in the absence of polycyclic aromatic hydrocarbon (PAH) molecules, which are ruled out as possible intermediaries (Jäger et al. 2009). Yet to date, no fullerene molecule has been detected in hot W-R stars in the most hydrogen-deficient R Coronae Borealis stars (García-Hernández et al. 2010) despite the expected efficiency of the formation process in such environments. Moreover, fullerenes are not expected to be formed in the hydrogen-rich circumstellar envelopes of cool, evolved stars (e.g., C-rich asymptotic giant branch (AGB) stars; Herwig 2005) and in the interstellar medium (De Vries et al. 1993), in spite of the fact that C-rich AGB stars are the sites of a complex and rich chemistry, with more than dozens of new complex molecules detected so far (Herbst & van Dishoeck 2009). In such cool, dense, and chemically rich conditions the acetylene (C₂H₂) and its radical derivatives are believed to be the precursors of more complex C-based molecules such as PAHs (Cherchneff & Cau 1999).

Slow, massive dust-driven mass loss at the end of the AGB leads to the formation of optically thick circumstellar envelopes. The surface chemistry of the AGB star (carbon- versus oxygen-rich based) is primarily a direct reflection of the stellar initial mass (which determines the number of dredge-up processes) and evolutionary stage (Herwig 2005). The planetary nebula (PN) phase starts with the photoionization of the circumstellar envelope and represents the immediate stage after the end of the AGB phase. The chemical mix of the ejecta from AGB dredge-up processes is not expected to be further modified during the PNe stage, apart from dust processing (Kwok et al. 2001). During the PNe stage however, fundamental chemical drivers are added into the system: the presence of a strong and evolving UV radiation field, and fast, tenuous winds that produce shocks.

The infrared detection of C₆₀ and C₇₀ fullerenes in the PN Tc 1 (Cami et al. 2010) has been reported recently. The authors state that the inner nebular regions of Tc 1 are carbon-rich, hydrogen-poor and dusty, and forwarded the hypothesis that Tc 1 underwent a late thermal pulse then presumably caused the ejection of this material, which now makes up the warm, dusty, and hydrogen-poor PN core where fullerenes are abundant. This interpretation is not supported by the literature. In fact, we note that neither the PN (Milanova & Kholtygin 2009; Köppen et al. 1991) nor its compact core (Williams et al. 2008; R. Williams 2010, private communication), and the central star (e.g., Mendez et al. 1988) of Tc 1 are H-poor. This evidence makes it very unlikely that Tc 1 underwent a final helium-shell flash (Iben et al. 1983) and that the environment where the fullerenes have been observed is thus hydrogen-poor. In addition, Tc 1 has a low-mass central star ($M_{\text{core}} = 0.54 M_{\odot}$; Maciel et al. 2008) and a slightly sub-solar metallicity (Perinotto et al. 1994), being identified as a slowly evolving type II PNe.

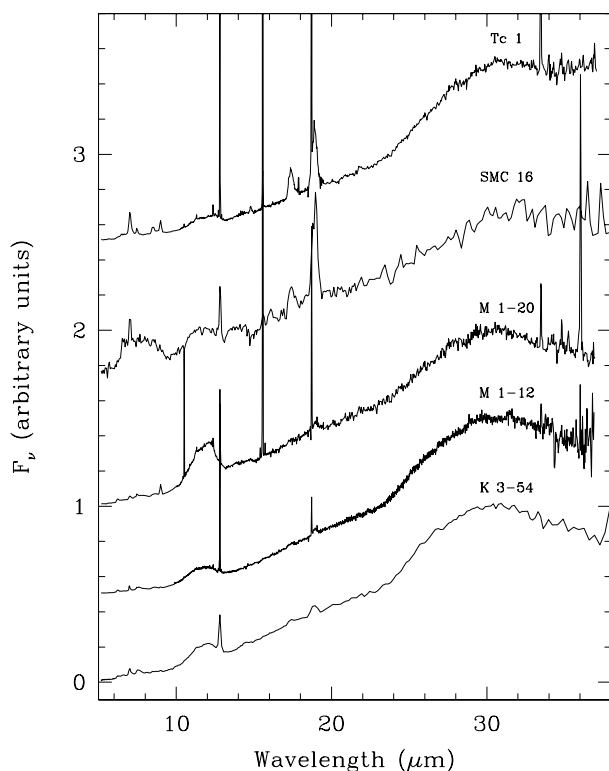


Figure 1. *Spitzer*/IRS spectra in the wavelength ~ 5 – $38 \mu\text{m}$ for the fullerene-detected PNe Tc 1, SMC SMP 16, M 1-20, M 1-12, and K 3-54. The spectra are normalized at $30 \mu\text{m}$ and displaced for clarity. Note that the strongest solid state C_{60} features at ~ 17.3 and $18.9 \mu\text{m}$ (Kratschmer et al. 1990) are clearly detected superimposed on the dust continuum thermal emission.

In this Letter, we present four new detections of C_{60} fullerenes together with PAHs and very small amorphous carbon grains in three Galactic and one Small Magellanic Cloud. H-containing PNe,⁹ challenging the current picture that the presence or absence of hydrogen in this type of carbon-rich environment clearly determines whether the chemical pathways favor the formation of PAH molecules or fullerenes as large aromatic species (Cami et al. 2010). The detection of fullerene in SMP SMC 16 reported in this Letter is the first such detection in an extragalactic source.

2. INFRARED SPECTRA OF FULLERENE-DETECTED PNe

The infrared spectra of the PNe M 1-20, M 1-12, K 3-54, and SMP SMC 16 presented here (see Figure 1) were all acquired with *Spitzer*/IRS under several General Observer programs. Program 3633 (PI: M. Bobrowsky) observed a sample of 40 PNe in the direction of the Galactic bulge (Perea-Calderón et al. 2009). Program 20443 (PI: L. Stanghellini) includes 157 compact Galactic disk PNe (L. Stanghellini et al. 2011, in preparation). Finally, program 50261 (PI: L. Stanghellini) was directed toward 41 extragalactic (thus low-metallicity PNe) in the Magellanic Clouds (Stanghellini et al. 2007; Shaw et al. 2010).¹⁰ All programs have a spectral coverage in the ~ 5 – $38 \mu\text{m}$ range in common, making use of different combinations of the Short-Low (SL: 5.2 – $14.5 \mu\text{m}$; $64 < R < 128$), Long-Low (LL:

14.0 – $38 \mu\text{m}$; $64 < R < 128$), Short-High (SH: 9.9 – $19.6 \mu\text{m}$; $R \sim 600$), and Long-High (LH: 18.7 – $37.2 \mu\text{m}$; $R \sim 600$) modules depending on the source brightness at mid-infrared wavelengths and assuring that a minimum signal-to-noise ratio of ~ 50 is usually reached. More detailed descriptions of the *Spitzer* observations and the data reduction process can be found in the relevant references and will not be repeated here. For comparison purposes, we also analyze the *Spitzer* spectrum of Tc 1 from program GO 3633, previously published (Perea-Calderón et al. 2009) in which solid state C_{60} and C_{70} fullerenes have been reported recently (Cami et al. 2010). Following the definitions of low, intermediate, and high excitation in PNe from infrared lines (Stanghellini et al. 2007), we determine that the targets with detected fullerene are all low-excitation PNe. All these PNe also show broad dust emission features centered at ~ 11.5 and $30 \mu\text{m}$ and generally attributed to SiC and MgS, respectively (Speck et al. 2009; Hony et al. 2002). The strongest solid state C_{60} features at ~ 17.3 and $18.9 \mu\text{m}$ (Kratschmer et al. 1990) are clearly detected superimposed on the dust continuum thermal emission (Figure 1).

In order to obtain the residual spectra, where dust and gas features may be easily identified, we have subtracted the dust continuum emission by fitting five order polynomials between 5 and $22 \mu\text{m}$ at spectral locations free from any dust or gas feature. We find that four PNe show strong fullerene C_{60} features at ~ 7.0 , 8.5 , 17.3 , and $18.9 \mu\text{m}$. This phenomenon is much more common than anyone thought and deserves much more attention to understand the implications. The four PNe containing fullerene have similarly low excitation, infrared spectral energy distributions, and carbon dust properties (Figure 1), and it has been shown (Stanghellini et al. 2007) that progenitors of PNe with similar characteristics typically are carbon-rich in the mid-to-lower end of the AGB mass sequence (~ 1 – $2 M_{\odot}$). Figure 2 shows that the C_{60} fullerene features are clearly detected in all sources. However, the strongest and isolated C_{70} features at ~ 12.6 and $14.9 \mu\text{m}$ are only tentatively detected in M 1-20 and M 1-12. We can neither confirm nor exclude the possibility of the latter C_{70} emission features in K 3-54 and in SMP SMC 16 given the much lower resolution in the *Spitzer* spectrum for these sources. The intriguing result is that all three Galactic PNe also show weak PAH features (e.g., those centered at ~ 6.2 , 7.7 , 8.6 , and $11.3 \mu\text{m}$). Note that three of the fullerene-detected PNe (K 3-54, M 1-12, and SMP SMC 16) are compact PNe ($< 4''$), and the spectral results represent the integration over the whole nebulae. However, M 1-20 is an extended PN (like Tc 1), and PAHs and fullerenes are observed together in the inner $4''$ region (the aperture of *Spitzer*). This seems to be in contrast with the conclusions of Cami et al. (2010), which associate the presence of fullerene features in the Tc 1 spectrum with a hydrogen-poor region of the PN. The detection of PAHs in the three Galactic PNe is highlighted in Figure 3, where an enlarged plot from 5 to $16 \mu\text{m}$ is shown.

3. MID-IR C_{60} FULLERENE FEATURES

Table 1 lists the wavelength position and width of the four C_{60} fullerene features as measured in the residual spectra. The derived positions and widths of the four neutral C_{60} features seen in M 1-20, M 1-12, K 3-54, and SMP SMC 16 compare very well with those seen in Tc 1. Note that the profiles, positions, and widths of the C_{60} bands indicate that C_{60} molecules are in a neutral state, being likely trapped on dust grains (Cami et al. 2010). The $\sim 7.0 \mu\text{m}$ feature is blended with an [Ar II] line but

⁹ The presence of hydrogen is demonstrated by the presence of PAHs and/or by the supporting available literature on these sources.

¹⁰ In total, the *Spitzer*/IRS spectra of ~ 240 PNe were inspected for the presence of the strongest features of the C_{60} and C_{70} complex species.

Table 1
Mid-IR C₆₀ Features^a in PNe

Feature	λ_{lab}^b (μm)	λ_{obs} (μm)	FWHM_{obs} (μm)	λ_{obs} (μm)	FWHM_{obs}						
	Tc 1		M 1-20		M 1-12		K 3-54		SMC 16		
$T_{1u}(4)$	7.00	7.03	0.193	7.02	0.178	6.99	0.092	7.03	0.344	7.02	0.129
$T_{1u}(3)$	8.45	8.51	0.240	8.58	0.343	8.58	0.237	8.50	0.686	8.56	0.309
$T_{1u}(2)$	17.33	17.39	0.372	17.35	0.470	17.37	0.357	17.38	0.463	17.42	0.614
$T_{1u}(1)$	18.94	18.89	0.394	18.96	0.412	18.94	0.348	18.86	0.484	18.92	0.456

Notes.

^a Positions and widths measured in the residual spectra. Note that the 7.0 μm C₆₀ band is blended with [Ar II] 6.99 μm .

^b Solid state laboratory data from Kratschmer et al. (1990).

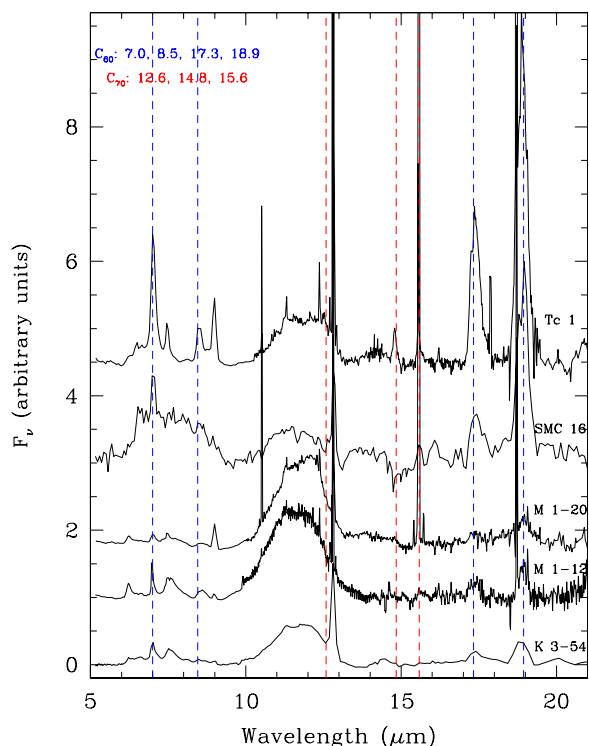


Figure 2. Residual spectra in the wavelength range $\sim 5\text{--}20\ \mu\text{m}$ for the PNe Tc 1, SMP SMC 16, M 1-20, M 1-12, and K 3-54. The wavelength positions of the solid state C₆₀ features (Kratschmer et al. 1990) are marked with blue dashed vertical lines. In addition, the strongest and unblended C₇₀ features (von Czarowski & Meiwes-Broer 1995) are marked with red dashed vertical lines.

(A color version of this figure is available in the online journal.)

the relative strengths of the other three neutral C₆₀ features at ~ 8.4 , 17.3, and 18.9 μm are similar for all sources. The C₆₀ molecule's excitation temperature from the population of the upper states of the four vibrational states are found to be about 425, 546, 681, and 326 K in M 1-20, M 1-12, K 3-54, and SMP SMC 16, respectively (see Cami et al. 2010 for more details about the method applied).¹¹ This means that the temperature of the C₆₀ molecules in the three Galactic PNe is higher than in Tc 1 (332 K) and that these molecules—which coexist with other carbon-based species like PAHs—are closer to the central star. However, the excitation temperature of C₆₀ in the extragalactic

¹¹ We note that if the 8.5 μm C₆₀ feature is contaminated by the PAH 8.6 μm band in the Galactic PNe M 1-20, M 1-12, and K 3-54, then slightly different temperatures would be obtained.

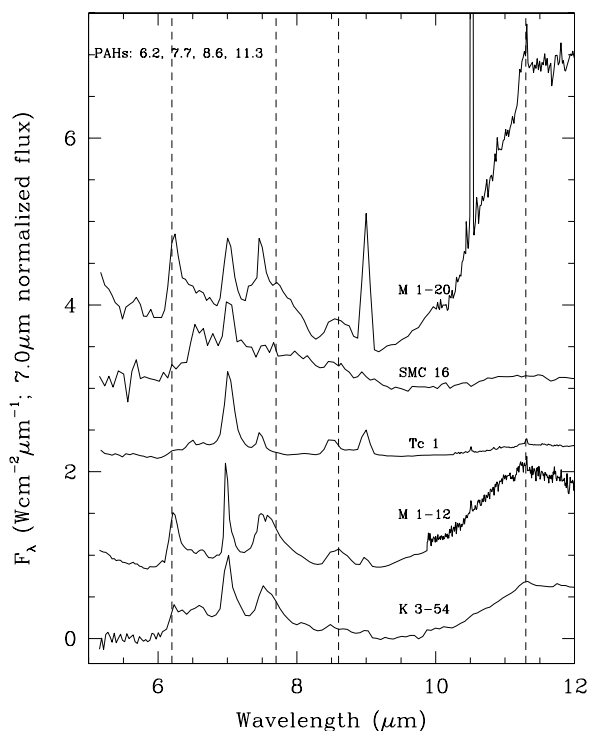


Figure 3. Residual spectra in the wavelength range $\sim 5\text{--}16\ \mu\text{m}$ for the PNe Tc 1, SMP SMC 16, M 1-20, M 1-12, and K 3-54. The wavelength positions of the classical PAH features (6.2, 7.7, 8.6, and 11.3 μm) are marked with black dashed vertical lines.

and low-metallicity PNe SMP SMC 16 is almost identical to that of Tc 1 (see Figure 4). Indeed, Tc 1 and SMP SMC 16 are infrared spectroscopic twins. The only difference is the clear presence of a broad 6–9 μm emission feature in SMP SMC 16 which is not seen in Tc 1 and attributable to hydrogenated amorphous carbon (HAC), very small grains, or PAH clusters (Tielens 2008; Buss et al. 1993; Rapacioli et al. 2005).

SMP SMC 16 offers the unique opportunity of obtaining a reliable estimation of the C₆₀ content in H-rich circumstellar ejecta because the distance to the Small Magellanic Cloud is known with good accuracy to be 61 kpc (Hilditch 2005), and because of the availability of a reliable C atomic abundance from UV spectra (Stanghellini et al. 2009). From the number of C₆₀ molecules,¹² a mass of $\sim 5.44 \times 10^{-7} M_{\odot}$ of pure C₆₀ is obtained. From the [S II] $\lambda\lambda 6717, 6731$ line fluxes

¹² We obtained a total number of 9×10^{47} C₆₀ molecules for the distance of 61 kpc (see Figure 4).

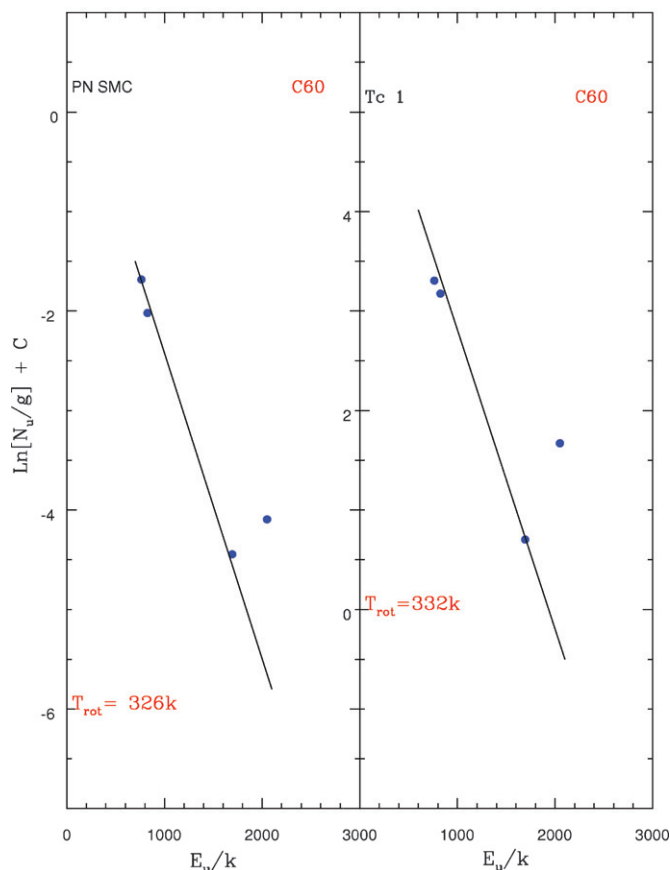


Figure 4. Illustrative example of the vibrational excitation temperature diagrams for the C_{60} bands observed in the PNe SMP SMC 16 (left panel) and Tc 1 (right panel).

(A color version of this figure is available in the online journal.)

(Shaw et al. 2006), we derived an electronic density n_e of 10^4 cm^{-3} . Combining this value with the observed H_β flux (Shaw et al. 2006) and the electronic temperature T_e of 11,800 K (Leisy & Dennefeld 2006), a hydrogen mass of $0.09 M_\odot$ is derived. Combining this mass with the carbon abundance (Stanghellini et al. 2009), a C mass of $\sim 1.72 \times 10^{-4} M_\odot$ is obtained. Therefore, C_{60} represents $\sim 0.32\%$ of the total carbon in SMP SMC 16. Our estimation is consistent with previous estimations for C_{60}^+ (e.g., Foing & Ehrenfreund 1994) from optical observations and a factor of five lower than the rather uncertain $\sim 1.5\%$ estimate in Tc 1 (Cami et al. 2010).

4. DISCUSSION

Our observations demonstrate that PAHs and fullerenes coexist in the circumstellar ejecta of low-excitation and H-containing PNe in our Galaxy and in the Small Magellanic Cloud. This observational result has profound implications on our understanding of the chemistry of large organic molecules and the possible routes of chemical processing in space, highlighting the question of how these large molecules are formed. This is a very difficult question. At present, the most likely explanation for the simultaneous presence of fullerenes and PAHs in H-containing environments is that they may be formed by the photochemical processing of HAC (Scott & Duley 1996; Scott et al. 1997a). The distribution of components in the mass spectra of products sputtered from HAC is found to show a complex dependence on the fluence and on the irradiation history

of the surface of the grains (Scott et al. 1997a), being consistent with the known sensitivity of HAC solids to thermal and photochemical modification (Duley 1993). The laboratory IR spectra (e.g., the relative strength of the IR features) of HACs are known to be strongly dependent on the physical conditions and HAC's chemical composition (Scott & Duley 1996; Scott et al. 1997a, 1997b; Grishko et al. 2001). In particular, laboratory studies (Grishko et al. 2001) show that HACs may explain the broad amorphous bands at ~ 21 , 26, and $30 \mu\text{m}$ —the latter feature sometimes very broad—observed in C-rich protoPNe and evolved PNe (Hony et al. 2002; Kwok et al. 1999; Hrivnak et al. 2000). Interestingly, all fullerene-detected PNe show the very broad $30 \mu\text{m}$ feature generally attributed to MgS (Hony et al. 2002). Thus, the broad $30 \mu\text{m}$ feature observed in the fullerene-detected PNe may be also related to HACs, which should be a major constituent in the circumstellar envelope.

Observationally, it is well known that the net result of the increasing UV irradiation from the AGB phase to the PNe stage is the transformation from aliphatic to aromatic groups (Kwok et al. 2001; García-Lario & Perea-Calderón 2003). Infrared emission spectra of HAC also show this progression in response to the thermal heating (Scott et al. 1997b; Duley 2000). In relatively massive C-rich sources, this process must be very fast and under more energetic conditions (e.g., a rapidly changing UV radiation field or strong post-AGB shocks). However, in low-excitation, low-mass C-rich objects, this process is postponed to the PNe stage (e.g., a slowly evolving UV irradiation and weak post-AGB shocks) and takes place slowly enough that we can see the HAC's decomposition products (both PAHs and fullerenes) being generated and coexisting all together. It is to be noted here that the C_{60} molecules seem to emit in the solid phase, being likely trapped on dust grains (Cami et al. 2010). Thus, the formation of fullerenes may be facilitated when the hydrogens have been removed from the surface of the carbonaceous grains. The de-hydrogenation of the grains is not the consequence of an H-poor environment, but of the photochemical processing of HACs. We believe that this is the case for the fullerene-detected PNe presented here, showing HACs and/or PAHs and fullerenes in their circumstellar envelopes. However, the possible evolutionary sequence of the HAC's decomposition products seen in the PNe is unclear. Laboratory experiments (Scott et al. 1997a) show that at low fluence conditions (e.g., like in our slowly evolving PNe), the dissolution of HACs occurs sequentially, with small molecules and molecular fragments being sputtered before heavier molecules and clusters. Future observations of a larger sample of slowly evolving PNe with different UV irradiation as well as laboratory spectroscopy of HAC films under very different physical conditions and chemical composition will help to solve this puzzle.

In summary, both PAHs and fullerenes may be formed by the decomposition of HAC (Scott & Duley 1996; Scott et al. 1997a). Hydrogen is needed to form HAC grains, which may be then destroyed by the central star's UV photons and/or by the post-AGB shocks. The products of destruction of HAC grains are PAHs and fullerenes in the form of C_{50} , C_{60} , and C_{70} molecules (Scott et al. 1997a). The C_{60} molecules may be hardy enough to survive for longer periods of time. This picture would explain why the C_{60} and C_{70} fullerenes in Tc 1 (Cami et al. 2010) are unaccompanied by HACs and PAHs. Indeed, the very low-excitation and low-metallicity PN SMP SMC 16 shows a fullerene-dominated spectrum with no signs of PAHs; the same is observed in its Galactic counterpart Tc 1.

In addition, this interpretation is supported by the recent detection of C₆₀ molecules (possibly in the gas phase) in the least H-deficient R Coronae Borealis stars DY Cen and V854 Cen (García-Hernández et al. 2010).¹³ Our detection of fullerenes in a variety of PNe that span a large range of progenitor's characteristics yet are narrowed down to a particular mid-infrared spectral type and in the typical presence of PAH features, will be an essential starting point to understand the photochemical processing of dust in circumstellar (and perhaps, interstellar) environments.

D.A.G.H acknowledges N. Kameswara Rao and David L. Lambert for the construction of the excitation diagrams and very interesting discussions. D.A.G.H. and A.M. acknowledge support for this work provided by the Spanish Ministry of Science and Innovation (MICINN) under a JdC grant and under grant AYA-2007-64748. Thanks to James Davies for helping in data analysis. This work is based on observations made with the *Spitzer Space Telescope*, which is operated by the Jet Propulsion Laboratory, California Institute of Technology, under NASA contract 1407. L.S. and R.A.S. acknowledge support by NASA through awards for programs GO 20443 and 50261 issued by JPL/Caltech. R.Sz. acknowledges support from grant N203 511838 from Polish MNiSW.

Facilities: Spitzer

REFERENCES

- Buss, R. H., et al. 1993, *ApJ*, 415, 250
 Cami, J., et al. 2010, *Science*, 329, 1180
 Cherchneff, I., & Cau, P. 1999, in IAU Symp. 191, Asymptotic Giant Branch Stars, ed. T. Le Betre, A. Lebre, & C. Waelkens (San Francisco, CA: ASP), 251
 Cherchneff, I., et al. 2000, *A&A*, 357, 752
 De Vries, M. S., et al. 1993, *Geochim. Cosmochim. Acta*, 57, 933
 Duley, W. W. 1993, in *Dust and Chemistry in Astronomy*, ed. T. J. Millar & D. A. Williams (Bristol: IOP Publishing), 71
 Duley, W. W. 2000, *ApJ*, 528, 841
 Foing, B. H., & Ehrenfreund, P. 1994, *Nature*, 369, 296
 García-Hernández, D. A., Rao, N. K., & Lambert, D. L. 2010, *ApJL*, submitted
 García-Lario, P., & Perea-Calderón, J. V. 2003, in *Exploiting the ISO Data Archive: Infrared Astronomy in the Internet Age*, ed. C. Gry et al. (ESA SP-511; Noordwijk: ESA), 97
 Goeres, A., & Sedlmayr, E. 1992, *A&A*, 265, 216
 Grishko, V. I., et al. 2001, *ApJ*, 558, L129
 Herbst, E., & van Dishoeck, E. F. 2009, *ARA&A*, 47, 427
 Herwig, F. 2005, *ARA&A*, 43, 435
 Hilditch, R. W. 2005, *MNRAS*, 357, 304
 Hony, S., et al. 2002, *A&A*, 390, 533
 Hrivnak, B. J., et al. 2000, *ApJ*, 535, 275
 Iben, I., Jr., et al. 1983, *ApJ*, 264, 605
 Jäger, C., et al. 2009, *ApJ*, 696, 706
 Köppen, J., et al. 1991, *A&A*, 248, 197
 Kratschmer, W., et al. 1990, *Nature*, 347, 354
 Kroto, H. W., et al. 1985, *Nature*, 318, 162
 Kwok, S., et al. 1999, *A&A*, 350, L35
 Kwok, S., et al. 2001, *ApJ*, 554, L87
 Leisy, P., & Dennefeld, M. 2006, *A&A*, 456, 451
 Maciel, W. J., et al. 2008, *RevMexAA*, 44, 221
 Mendez, R. H., et al. 1988, *A&A*, 190, 113
 Milanova, Yu. V., & Kholtygin, A. F. 2009, *Astron. Lett.*, 35, 518
 Perea-Calderón, J. V., et al. 2009, *A&A*, 495, L5
 Perinotto, M., et al. 1994, *A&A*, 107, 481
 Rapacioli, M., et al. 2005, *A&A*, 429, 193
 Scott, A. D., & Duley, W. W. 1996, *ApJ*, 472, L123
 Scott, A. D., et al. 1997a, *ApJ*, 489, L193
 Scott, A. D., et al. 1997b, *ApJ*, 490, L175
 Shaw, R. A., et al. 2006, *ApJS*, 167, 201
 Shaw, R. A., et al. 2010, *ApJ*, 717, 562
 Speck, A., et al. 2009, *ApJ*, 691, 1202
 Stanghellini, L., et al. 2007, *ApJ*, 671, 1669
 Stanghellini, L., et al. 2009, *ApJ*, 702, 733
 Tielens, A. G. G. M. 2008, *ARA&A*, 46, 289
 von Czarowski, A., & Meiwes-Broer, K. H. 1995, *Chem. Phys. Lett.*, 246, 321
 Wang, X. K., et al. 1995, *J. Mater. Res.*, 10, 1977
 Williams, R., et al. 2008, *ApJ*, 677, 1100

¹³ The recent non-detection of C₆₀ across the R Coronae Borealis stars sample (except for the least H-deficient stars DY Cen and V854 Cen with H-deficiencies of ~10–100 only) is additional evidence that C₆₀ is not easily (or at all) formed in H-poor environments (García-Hernández et al. 2010).